

# Polarization analysis of K-edge resonant x-ray scattering of germanium

C. Detlefs

*European Synchrotron Radiation Facility, Boîte Postale 220, 38043 Grenoble, Cedex, France.*

(Dated: March 22, 2022)

The polarization of K-edge resonant scattering at the space group “forbidden”  $(0\ 0\ 6)$  reflection of Ge was measured as function of the azimuthal angle,  $\psi$ . The experimental results are compared to model calculations based on symmetry analysis of the resonant scattering tensors.

PACS numbers: 61.10.Dp, 61.10.Eq, 78.70.Ck

In the last few years the investigation of resonant scattering phenomena has allowed novel studies of antiferromagnetism (through resonant magnetic x-ray scattering<sup>1</sup>) and, more recently, of orbital<sup>2,3,4,5</sup> and quadrupolar order<sup>6</sup>. Although much progress has been made in the theory and interpretation of these effects, a large number of open questions concerning the origin of the scattering remains.

A characteristic feature of resonant scattering is its polarization dependence, which differs markedly from that of normal Thompson scattering. Indeed, polarization analysis (PA) has now been developed into a standard tool for the study of the aforementioned effects. In this communication I present a study of resonant x-ray scattering at the Ge K-edge with emphasis on the analysis of polarization effects. Anisotropic tensor susceptibility (ATS) scattering<sup>7,8,9</sup> and orbital/quadrupolar order resonances are intimately related as the scattering arises from the same transitions between core level and valence band electronic states<sup>10</sup>. Therefore systematic studies of a well-known reference system may lead to better understanding of the complex situation in compounds exhibiting orbital order.

One may distinguish three different classes of ATS scattering, depending on the rank of the scattering tensor: The original experiment on  $\text{NaBrO}_3$  may be described by second rank tensors corresponding to electric dipole (E1) transitions<sup>7,8,9</sup>. A later experiment on  $\alpha\text{-Fe}_2\text{O}_3$  evidenced electric quadrupole (E2) transitions, which give rise to fourth rank tensors<sup>11</sup>. Finally, ATS scattering in Ge was attributed to rank three tensors. Two different origins of this tensor were proposed: An E1–E2 mixed resonance<sup>12,13,14</sup>, and an E1–E1 process combined with a displacement of the scattering atom due to thermal motion<sup>15,16</sup>. The subject is still under discussion<sup>17,18</sup>.

The azimuthal dependence of the scattered beam intensity was calculated and experimentally verified by Templeton and Templeton<sup>12</sup>, but without polarization analysis. For some selected photon energies, the phase of the  $(0\ 0\ 6)$  and  $(2\ 2\ 2)$  resonant scattering was determined by Lee et al.<sup>19</sup> through the interference with Umweg reflections. Finally, Kokubun et al.<sup>15</sup> and Kirfel et al.<sup>16</sup> studied the temperature dependence of the  $(0\ 0\ 2)$  and  $(0\ 0\ 6)$  resonant scattering. They observed a strong increase of the intensity with increasing temperature, but only minor variations in the line shape of the resonance.

They concluded that the dominant origin of resonant scattering lies in anisotropic thermal motion of the Ge atoms.

The aim of the present experiment was to complement the existing body of experimental data to further study resonant x-ray scattering of odd-rank tensors. Presented below are measurements of the resonant line shape and the azimuthal dependence of the polarization of the  $(0\ 0\ 6)$  reflection, which is forbidden by the glide-plane extinction rule.

The experiment was performed at the magnetic scattering beamline, ID20, of the ESRF. The scattering geometry was vertical, with incident  $\sigma$  polarization. A single crystal of Ge with a polished  $(0\ 0\ L)$  surface normal was mounted in the azimuthal scan configuration which allows to turn the sample about the scattering vector,  $\mathbf{Q}$ . The diffracted beam was reflected by a  $\text{Au}(3\ 3\ 3)$  polarization analyzer (PA) with  $2\theta_{\text{PA}} \approx 90^\circ$ , which also rejected fluorescence and other diffuse background. The PA may be rotated about the diffracted beam (angle  $\eta$ ).  $\eta = 0$  when the diffraction planes of the PA and the sample coincided, i.e. when the PA accepted  $\sigma'$  polarization.

Fig. 1 (top) shows the intensity of the  $(0\ 0\ 6)$  reflection as function of the incident photon energy. For each energy, the intensity was determined by integrating a rocking scan after subtraction of a constant background. To avoid contamination by strong Umweg reflections the energy dependence was measured in several scans at different azimuthal angles. Regions where a marked azimuthal dependence on was observed were rejected. No absorption correction was applied. The fluorescence yield and the intensity of the strong, allowed  $(0\ 0\ 4)$  reflection are shown in Fig. 1(bottom) for comparison.

Several features of these data are worth further discussion: Significant intensity is observed below the edge. This scattering may be due to the tails of Umweg reflections<sup>20</sup>, or to non-resonant ATS scattering<sup>21,22</sup>. Furthermore, two deep minima (indicated by the arrows in Fig. 1), below and above the main resonance are observed. Such minima are characteristic of a change of sign of the scattering amplitude and might indicate interference between resonant and non-resonant contributions. It would therefore be of interest to determine the phase of the resonant scattering, e.g. through interference with an Umweg reflection of known phase<sup>19,20</sup>. Finally, towards higher energies oscillations reminiscent of DAFS (Diffraction Anomalous Fine Structure) set in.

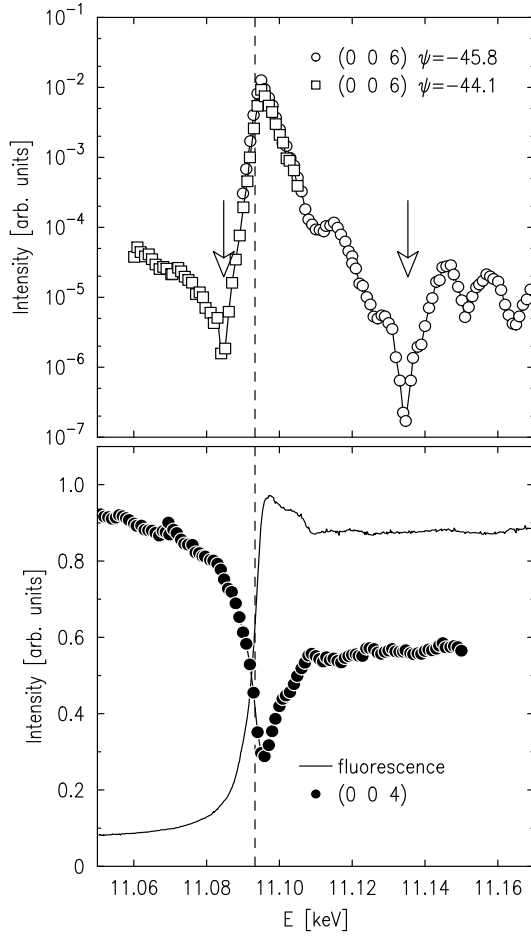


FIG. 1: Energy scans through the Ge K absorption edge, with the PA set at  $\eta = 0$ . The scattering at the forbidden (0 0 6) reflection shows a sharp resonance (top) near the inflection point of the absorption, as determined from measurements of the fluorescence and the (0 0 4) Bragg peak (bottom). The dashed line indicates the inflection point of the fluorescence curve.

For the polarization measurements discussed in the remainder of this Communication the photon energy was tuned to the maximum of the resonance at  $E = 11.096$  keV.

Fig. 2 shows the detected intensity as a function of the orientation of the PA for different azimuthal angles,  $\psi$ . For each  $\psi$ , the Ge(0 0 6) reflection was carefully aligned, and it was verified that there was no Umweg excitation in the immediate vicinity. This requirement resulted in slightly irregular values of  $\psi$ . The sample was then kept in this position while the polarization of the scattered beam was measured by rocking the analyzer crystal for settings of  $\eta$  between  $0^\circ$  and  $180^\circ$ . The integrated intensities of these rocking scans are shown as open circles in Fig. 2. The data for each  $\psi$  are normalized so that they are independent of the intensity of the scattered beam. Reliable measurements of the intensity of the scattered beam proved difficult in the present experimental setup,

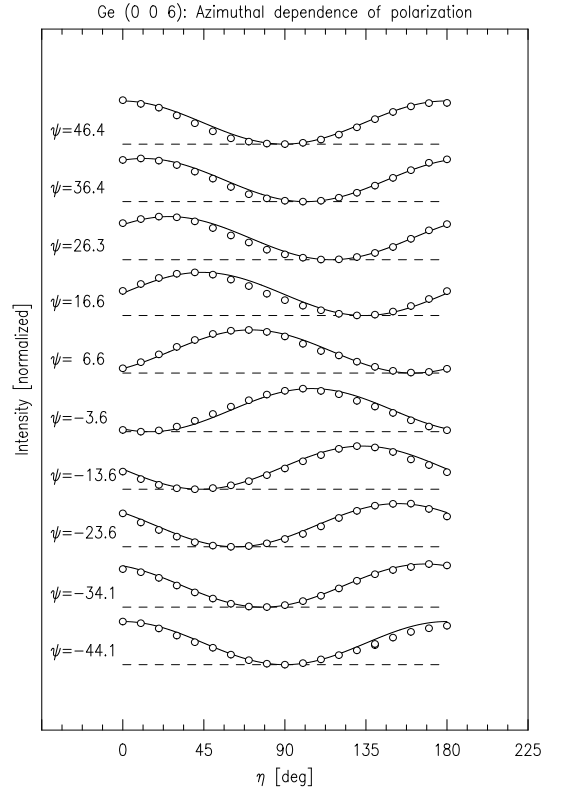


FIG. 2: Integrated intensities as function of the PA angle,  $\eta$ , for different azimuthal angles,  $\psi$ . All data are taken at  $E = 11.096$  keV. Each open circle represents the intensity obtained by integrated a rocking scan of the analyzer crystal. The solid lines represent model calculation based in eqs. 19, 20, and 4.

as the resolution function is determined by the combined narrow angular acceptances of the sample and the analyzer.

The polarization of an x-ray beam is most conveniently described by the Stokes parameters<sup>23</sup>,

$$P_1 = \frac{|F_{\sigma\sigma'}|^2 - |F_{\sigma\pi'}|^2}{|F_{\sigma\sigma'}|^2 + |F_{\sigma\pi'}|^2} \quad (1)$$

$$P_2 = \frac{|F_{\sigma\sigma'} + F_{\sigma\pi'}|^2 - |F_{\sigma\sigma'} - F_{\sigma\pi'}|^2}{2(|F_{\sigma\sigma'}|^2 + |F_{\sigma\pi'}|^2)} \quad (2)$$

$$P_3 = \frac{|F_{\sigma\sigma'} + iF_{\sigma\pi'}|^2 - |F_{\sigma\sigma'} - iF_{\sigma\pi'}|^2}{2(|F_{\sigma\sigma'}|^2 + |F_{\sigma\pi'}|^2)} \quad (3)$$

The dependence of the transmission of an idealized linear PA on these is given by

$$I(\eta) \propto [1 + P_1 \cos(2\eta) + P_2 \sin(2\eta)] \quad (4)$$

The data presented in Fig. 2 were fitted to eq. 4 in order to determine the dependence of the Stokes parameters,  $P_1$  and  $P_2$ , on  $\psi$ . The results are shown in Fig. 3. While the degree of circular polarization,  $P_3$ , was not directly measured, it vanishes because  $|P_3| \leq 1 - \sqrt{P_1^2 + P_2^2} \approx 0$ .

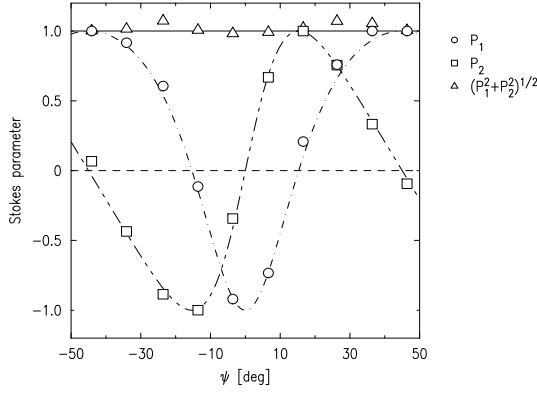


FIG. 3: Stokes parameters,  $P_{1,2}$  determined from fits of the intensities to eq. 4, compared to the model, eqs. 19 and 20.

As pointed out above, the dependence of the polarization on the azimuthal angle may be calculated from symmetry principles alone.

In Ge the two sites within the primitive unit cell are related by an inversion center at the midpoint of the covalent bond. As even rank tensors are invariant under space inversion, the aforementioned E1 and E2 resonances do not contribute to scattering at “forbidden” reflections,  $(HKL)$  with  $H + K + L = 4n + 2$ . An odd rank tensor is therefore needed to explain resonant scattering observed at forbidden reflections<sup>12,13,14</sup>.

The E1–E2 process<sup>12,13,14</sup> directly gives rise to third rank tensors,  $A_{\alpha\beta\gamma}$ . The resulting atomic scattering amplitude may be written as<sup>10</sup>

$$F(\mathbf{k}, \epsilon, \mathbf{k}', \epsilon') \propto \epsilon'_\alpha \epsilon_\beta [A_{\alpha\beta\gamma} k_\gamma - A'_{\alpha\beta\gamma} k'_\gamma] \quad (5)$$

with

$$A_{\alpha\beta\gamma} = \sum_{a,b} B^{(a,b)}(\hbar\omega) C_{\alpha\beta\gamma}^{(a,b)} \quad (6)$$

$$A'_{\alpha\beta\gamma} = \sum_{a,b} B^{(a,b)}(\hbar\omega) C_{\beta\alpha\gamma}^{(a,b)*} \quad (7)$$

$$B^{(a,b)}(\hbar\omega) = \frac{p_a}{E_a - E_b + \hbar\omega + i\Gamma/2} \quad (8)$$

$$C_{\alpha\beta\gamma}^{(a,b)} = \langle a | r_\alpha | b \rangle \langle b | r_\beta r_\gamma | a \rangle, \quad (9)$$

where  $\epsilon$  ( $\epsilon'$ ) and  $k$  ( $k'$ ) are the polarization and wave vectors of the incident (scattered) beam.  $|a\rangle$  and  $|b\rangle$  are the initial (=final) and intermediate electronic states.  $\hbar\omega$  is the photon energy, and  $\Gamma$  the inverse life time of the excited state.  $p_a$  is the probability that the corresponding state is occupied.

In a system that is invariant under time reversal states which are related by time reversal,  $|\bar{a}\rangle = T|a\rangle$ , have the same energy,  $E_{\bar{a}} = E_a$ , and probability of being occupied,  $p_{\bar{a}} = p_a$ , so that  $B^{(\bar{a},\bar{b})} = B^{(a,b)}$ . Furthermore,  $\langle \bar{a} | r_\alpha | \bar{b} \rangle = \langle b | r_\alpha | a \rangle$  and  $\langle \bar{a} | r_\beta r_\gamma | \bar{b} \rangle = \langle b | r_\beta r_\gamma | a \rangle$ , so that  $C_{\alpha\beta\gamma}^{(\bar{a},\bar{b})} = C_{\alpha\beta\gamma}^{(a,b)*}$ . The sum over  $a$  and  $b$  may equally

well be carried out over  $\bar{a}$  and  $\bar{b}$ , therefore<sup>10</sup>

$$A_{\alpha\beta\gamma} = \frac{1}{2} \sum_{a,b} B^{(a,b)}(\hbar\omega) [C_{\alpha\beta\gamma}^{(a,b)} + C_{\alpha\beta\gamma}^{(\bar{a},\bar{b})}] \quad (10)$$

$$= \sum_{a,b} B^{(a,b)}(\hbar\omega) \Re(C_{\alpha\beta\gamma}^{(a,b)}) \quad (11)$$

$$A'_{\alpha\beta\gamma} = A_{\beta\alpha\gamma}, \quad (12)$$

where  $\Re(x)$  denotes the real part of  $x$ . With this, eq. 5 reduces to

$$F(\mathbf{k}, \epsilon, \mathbf{k}', \epsilon') \propto \epsilon'_\alpha \epsilon_\beta [A_{\alpha\beta\gamma} k_\gamma - A_{\beta\alpha\gamma} k'_\gamma] \quad (13)$$

$$= \epsilon'_\alpha \epsilon_\beta [-(A_{\alpha\beta\gamma} + A_{\beta\alpha\gamma}) Q_\gamma + (A_{\alpha\beta\gamma} - A_{\beta\alpha\gamma})(k_\gamma + k'_\gamma)], \quad (14)$$

where  $\mathbf{Q} = (HKL) = \mathbf{k}' - \mathbf{k}$  is the scattering vector. The first term was already discussed by Templeton and Templeton<sup>12</sup>. The second term does not necessarily vanish in all cases — in fact, for certain symmetries it may lead to x-ray natural circular dichroism, XNCD<sup>24</sup>.

A different explanation for the origin of resonant scattering in Ge, termed Thermal Motion Induced (TMI) scattering, was recently proposed by Dmitrienko and Ovchinnikova<sup>25</sup>. Their theory constructs a rank 3 tensor from E1 transitions combined with a displacement of the scattering atom out of the crystallographic, high symmetry position. These displacements are assumed to be of thermal origin, so that the scattered intensity increases strongly with rising temperature. This increase has indeed been observed experimentally<sup>15,16</sup>.

In K-edge resonances an electron is promoted from a  $1s_{1/2}$  core level into an *unoccupied* valence band. The E1 and E2 selection rules require  $\Delta l = 1$  and  $\Delta l = 2$ , respectively. Consequently, the E1–E2 mixed and TMI resonances differ in their sensitivity to the conduction band symmetry: The former probes only valence bands with contributions of both  $p$  and  $d$  character, while the latter requires  $p$  character, only. In both cases band structure calculations are needed to obtain the spectral shape of the resonance<sup>13,14</sup>.

However, as pointed out above, detailed knowledge of the matrix elements is not necessary to calculate the polarization properties of the resonances. It suffices to require that  $A_{\alpha\beta\gamma}$  is invariant under the point group of the scattering site,  $T_d$  for the case of Ge. The resulting tensor is  $A_{\alpha\beta\gamma} = DT_{\alpha\beta\gamma}$ , where  $D$  is a complex number depending of the matrix elements, the resonant denominators, the densities of state, etc, but not on the scattering geometry, and the photon polarization and wave vectors.  $T_{\alpha\beta\gamma}$  is symmetric over all its indices, i.e.,  $T_{xyz} = T_{xzy} = T_{yzx} = T_{yxz} = T_{zxy} = T_{zyx} = 1$  and 0 otherwise<sup>16</sup>. In particular,  $A_{\alpha\beta\gamma}$  is symmetric in  $\alpha$  and  $\beta$ , so that the second term in eq. 14 vanishes, whereas the first term gives

$$F \propto D \epsilon'^* \cdot \begin{pmatrix} 0 & L & K \\ L & 0 & H \\ K & H & 0 \end{pmatrix} \cdot \epsilon. \quad (15)$$

Eq. 15 describes the third-rank tensor resonant contribution to any Bragg reflection. In general, this contribution is much smaller than the Thompson scattering. For practical purposes this term is therefore significant only when the Thompson contribution vanishes, i.e., at reflections which are “forbidden” due to glide plane or screw axis extinction rules, or structure factor arithmetic<sup>12</sup>.

For (0 0  $L$ )-type reflections of Ge, the anomalous resonant scattering amplitude is proportional to

$$F \propto D Q \left( \epsilon_1'^\dagger \epsilon_2 + \epsilon_2'^\dagger \epsilon_1 \right), \quad (16)$$

where the polarization vectors have to be transformed into the coordinate system of the crystal, i.e., the dependence on  $\psi$  is implicit in  $\epsilon$  and  $\epsilon'$ .

The polarization of the scattered beam is completely described by the scattering amplitudes into the channels with polarization perpendicular ( $\sigma'$ ) and parallel ( $\pi'$ ) to the scattering plane. For incident  $\sigma$  polarization they are

$$F_{\sigma\sigma'}(\theta, \psi) = D Q \sin(2\psi) \quad (17)$$

$$F_{\sigma\pi'}(\theta, \psi) = D Q \sin(\theta) \cos(2\psi), \quad (18)$$

with  $\psi = 0$  when the azimuthal reference vector, chosen as  $\mathbf{h}_0 = (1 \ 0 \ 0)$ , lies within the scattering plane.

Equations 17 and 18 yield the Stokes parameters

$$P_1(\theta, \psi) = \frac{\sin^2(2\psi) - \sin^2(\theta) \cos^2(2\psi)}{\sin^2(2\psi) + \sin^2(\theta) \cos^2(2\psi)} \quad (19)$$

$$P_2(\theta, \psi) = \frac{\sin(4\psi) \sin(\theta)}{\sin^2(2\psi) + \sin^2(\theta) \cos^2(2\psi)} \quad (20)$$

$$P_3(\theta, \psi) = 0. \quad (21)$$

This result is identical to that of Elfimov et al.<sup>14</sup>, obtained from band structure calculations. Note that  $P_{1,2,3}$  are independent of the scaling factor,  $D$ , and that  $P_1^2 + P_2^2 = 1$  for all  $\psi$ . The scattered beam is therefore always linearly polarized. The experimental data, shown in Fig. 3, agree well with the values calculated from eqs. 19 and 20 — bearing in mind that there are no adjustable parameters.

In summary, I have presented measurements of the polarization of ATS scattering at the forbidden (0 0 6) reflection of Ge. The dependence of the Stokes parameters  $P_1$  and  $P_2$  on the azimuthal angle,  $\psi$ , is well described by the model of third-rank scattering tensors. The line shape of the resonance was measured over an extended energy range.

In high symmetry systems such as this one, symmetry analysis of the scattering tensor allows detailed predictions about variation of the scattered intensity and polarization with the azimuthal angle. The technique is therefore particularly well adapted to the study of orbitally ordered systems, where the determination of the symmetry of the order parameter is a problem of fundamental importance.

#### Acknowledgments

Discussions with E. Lorenzo-Diaz, G. Sawatzky and L. Paolasini are gratefully acknowledged. Furthermore, I thank K. D. Finkelstein for critical reading of the manuscript and helpful comments.

- 
- <sup>1</sup> D. Gibbs, D. R. Harshman, E. D. Isaacs, D. B. McWhan, D. Mills, and C. Vettier, *Phys. Rev. Lett.* **61**, 1241 (1988).
  - <sup>2</sup> Y. Murakami et al., *Phys. Rev. Lett.* **81**, 582 (1998).
  - <sup>3</sup> L. Paolasini et al., *Phys. Rev. Lett.* **82**, 4719 (1999).
  - <sup>4</sup> D. F. McMorrow et al., *Phys. Rev. Lett.* **87**, 057201 (2001).
  - <sup>5</sup> J. A. Paixão, C. Detlefs, M. J. Longfield, P. Santini, N. Bernhoeft, J. Rebizant, and G. H. Lander, *Phys. Rev. Letters* **89**, 187202 (2002).
  - <sup>6</sup> K. Hirota, N. Oumi, T. Matsumura, H. Nakao, Y. Wakabayashi, Y. Murakami, and Y. Endoh, *Phys. Rev. Lett.* **84**, 2706 (2000).
  - <sup>7</sup> D. H. Templeton and L. K. Templeton, *Acta Crystallogr. A* **41**, 133 (1985).
  - <sup>8</sup> V. E. Dmitrienko, *Acta Crystallogr. A* **39**, 29 (1983).
  - <sup>9</sup> V. E. Dmitrienko, *Acta Crystallogr. A* **40**, 89 (1984).
  - <sup>10</sup> M. Blume, in *Resonant anomalous x-ray scattering*, edited by G. Materlik, C. J. Sparks, and K. Fischer (Elsevier Science, Amsterdam, 1994), p. 495.
  - <sup>11</sup> K. D. Finkelstein, Q. Shen, and S. Shastri, *Phys. Rev. Lett.* **69**, 1612 (1992).
  - <sup>12</sup> D. H. Templeton and L. K. Templeton, *Phys. Rev. B* **49**, 14850 (1994).
  - <sup>13</sup> I. S. Elfimov, N. A. Skorikov, V. I. Anisimov, and G. A. Sawatzky, *Phys. Rev. Lett.* **88**, 015504 (2002).
  - <sup>14</sup> I. S. Elfimov, N. A. Skorikov, V. I. Anisimov, and G. A. Sawatzky, *Phys. Rev. Lett.* **88**, 239904(E) (2002).
  - <sup>15</sup> J. Kokubun, M. Kanazawa, K. Ishida, and V. E. Dmitrienko, *Phys. Rev. B* **64**, 073203 (2001).
  - <sup>16</sup> A. Kirfel, J. Grybox, and V. E. Dmitrienko, *Phys. Rev. B* **66**, 165202 (2002).
  - <sup>17</sup> V. E. Dmitrienko and K. Ishida, *Phys. Rev. Lett.* **90**, 129601 (2003), comment on Ref. 13.
  - <sup>18</sup> I. S. Elfimov, N. A. Skorikov, V. I. Anisimov, and G. A. Sawatzky, *Phys. Rev. Lett.* **90**, 129602 (2003), reply to Ref. 17.
  - <sup>19</sup> T. L. Lee et al., *Phys. Rev. B* **64**, R201316 (2001).
  - <sup>20</sup> J. Z. Tischler and B. W. Batterman, *Acta Crystallogr. A* **42**, 510 (1986).
  - <sup>21</sup> M. Amara and P. Morin, *J. Phys.: Condens. Matter* **10**, 9875 (1998).
  - <sup>22</sup> M. Amara, S. E. Luca, and R. M. Galéra, *J. Phys.: Condens. Matter* **13**, 9621 (2001).
  - <sup>23</sup> F. W. Lipps and H. A. Tolhoek, *Physica* **20**, 85 (1954).
  - <sup>24</sup> J. Goulon et al., *J. Chem. Phys.* **108**, 6394 (1998).
  - <sup>25</sup> V. E. Dmitrienko and E. N. Ovchinnikova, *Acta Crystallogr. A* **56**, 340 (2000).